Observational Constraints for Modeling Diffuse Molecular Clouds

S. R. Federman

Department of Physics and Astronomy, University of Toledo, MS 111, Toledo, 43606 OH USA
email: `steven.federman@utoledo.edu`

Abstract. Ground-based and space-borne observations of diffuse molecular clouds suggest a number of areas where further improvements to modeling efforts is warranted. I will highlight those that have the widest applicability. The range in CO fractionation caused by selective isotope photodissociation, in particular the large $^{12}C^{16}O/^{13}C^{16}O$ ratios observed toward stars in Ophiuchus, is not reproduced well by current models. Our ongoing laboratory measurements of oscillator strengths and predissociation rates for Rydberg transitions in CO isotopologues may help clarify the situation. The CH^+ abundance continues to draw attention. Small scale structure seen toward ζ Per may provide additional constraints on the possible synthesis routes. The connection between results from optical transitions and those from radio and sub-millimeter wave transitions requires further effort. A study of OH^+ and OH toward background stars reveals that these species favor different environments. This brings to focus the need to model each cloud along the line of sight separately, and to allow the physical conditions to vary within an individual cloud, in order to gain further insight into the chemistry. Now that an extensive set of data on molecular excitation is available, the models should seek to reproduce these data to place further constraints on the modeling results.

Keywords. ISM: abundances, ISM: molecules, astrochemistry
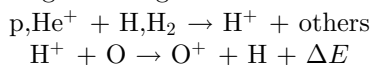
1. Introduction

Detailed models of diffuse molecular clouds were first developed over thirty years ago (e.g., Glassgold & Langer 1974, 1976; Black & Dalgarno 1977; van Dishoeck & Black 1986). Two key ingredients to these and subsequent models are ion-molecule reactions and photochemistry. Major advances in the more recent past involve ground-based and space-based observations with improved sensitivity. Instrumentation now provides molecular abundances for more reddened lines of sight, for species more complex than simple diatomics (such as H_2, CH, CH^+, CN, and CO known to exist before 1980), and for less abundant species including NH, OH^+, and H_2O^+ that are important intermediates in the chemical models.

Here I describe a number of these developments and how they inform us about directions toward more sophisticated models. The next Section describes recent CO measurements acquired at ultraviolet wavelengths with the *Hubble Space Telescope* and the *Far Ultraviolet Spectroscopic Explorer* as well as supporting experimental results for modeling CO photochemistry. Related observations on the isotopologues of CH^+ and CN are also discussed here. Section 3 presents new work on small scale structure in the diffuse molecular cloud toward ζ Per and the constraints it places on the synthesis of CH^+. This is followed by a discussion on OH^+ and OH chemistry in Section 4 and molecular excitation in Section 5. The final section describes necessary improvements to models so that they can incorporate these new results.
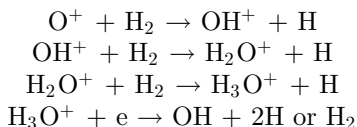
321

2. CO Photochemistry

Detailed studies of the abundance of CO and the ratio of isotopologues in diffuse molecular clouds include those of Sheffer *et al.* (2002b, 2007, 2008), Pan *et al.* (2005), and Sonnentrucker *et al.* (2007). As noted by Sheffer *et al.* (2008), the pathways to the production of CO involve the following sequence of reactions (e.g., Glassgold & Langer 1976).
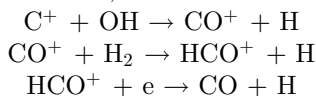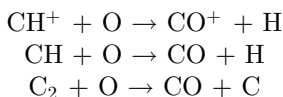
Cosmic ray ionization and charge exchange
$$\text{p,He}^+ + \text{H,H}_2 \rightarrow \text{H}^+ + \text{others}$$
$$\text{H}^+ + \text{O} \rightarrow \text{O}^+ + \text{H} + \Delta E$$
Hydrogen abstraction and dissociative recombination
$$\text{O}^+ + \text{H}_2 \rightarrow \text{OH}^+ + \text{H}$$
$$\text{OH}^+ + \text{H}_2 \rightarrow \text{H}_2\text{O}^+ + \text{H}$$
$$\text{H}_2\text{O}^+ + \text{H}_2 \rightarrow \text{H}_3\text{O}^+ + \text{H}$$
$$\text{H}_3\text{O}^+ + \text{e} \rightarrow \text{OH} + 2\text{H or H}_2$$
Carbon insertion, hydrogen abstraction, and dissociative recombination
$$\text{C}^+ + \text{OH} \rightarrow \text{CO}^+ + \text{H}$$
$$\text{CO}^+ + \text{H}_2 \rightarrow \text{HCO}^+ + \text{H}$$
$$\text{HCO}^+ + \text{e} \rightarrow \text{CO} + \text{H}$$
Other (minor) channels
$$\text{CH}^+ + \text{O} \rightarrow \text{CO}^+ + \text{H}$$
$$\text{CH} + \text{O} \rightarrow \text{CO} + \text{H}$$
$$\text{C}_2 + \text{O} \rightarrow \text{CO} + \text{C}$$

The difference in ionization potentials for H and O is $E/k \approx 232$ K. This set of reactions incorporated into the Cloudy code adequately describes the trends seen in a plot of log $N(\text{CO})$ versus log $N(\text{H}_2)$ (Sheffer *et al.* 2008). For low column densities, CO production is initiated by $\text{CH}^+ + \text{O}$, while for higher column densities, a combination of production via $\text{C}^+ + \text{OH}$, higher gas densities $[n(\text{H}) + 2\,n(\text{H}_2)]$, and self shielding are important.

Fractionation among the isotopologues of CO arises from two processes. Isotope charge exchange (Watson *et al.* 1976), $^{13}\text{C}^+ + {}^{12}\text{C}^{16}\text{O} \rightarrow {}^{12}\text{C}^+ + {}^{13}\text{C}^{16}\text{O}$, favors $^{13}\text{C}^{16}\text{O}$ because it has a lower zero-point energy. Selective isotope photodissociation (e.g., Bally & Langer 1982) leads to enhancements in the more abundant variants, such as $^{12}\text{C}^{16}\text{O}$. This arises because CO photodissociation involves line absorption: the more abundant forms of CO have lines with larger optical depths, effectively shielding molecules deeper in the cloud. This self shielding and mutual shielding from H_2 was modeled in detail by van Dishoeck & Black (1988) and Visser *et al.* (2009).

Observations with the *Hubble Space Telescope* provided the basis for many of the studies on CO fractionation in diffuse molecular clouds. Lambert *et al.* (1994) and Federman *et al.* (2003) found significant enhancements in $^{12}\text{C}^{16}\text{O}$ toward stars in Ophiuchus, indicating the effectiveness of self shielding. More recent work (e.g., Sheffer *et al.* 2002b, 2007; Sonnentrucker *et al.* 2007) expanded the number of sight lines examined. Sheffer *et al.* (2002b) detected $^{12}\text{C}^{18}\text{O}$ and $^{12}\text{C}^{17}\text{O}$ toward X Per and found self shielding was affecting the C-bearing isotopologues but not the less abundant O-bearing ones. The most comprehensive study to date (Sheffer *et al.* 2007) focused on the C-bearing variants. This survey revealed directions where charge exchange dominates and others where self shielding is important, but most of the sample had a $N(^{12}\text{C}^{16}\text{O})/N(^{13}\text{C}^{16}\text{O})$ ratio ≈ 70, the ambient $^{12}\text{C}/^{13}\text{C}$ ratio in the solar neighborhood based on millimeter-wave observations of dark cloud cores (e.g., Wilson 1999). (More about the ambient ratio appears below.)

A plot of $N(^{12}C^{16}O)/N(^{13}C^{16}O)$ versus $N(^{12}C^{16}O)$ indicates where the various fractionation processes take place (Sheffer *et al.* 2007 – see their Fig. 7). Self shielding for $^{12}C^{16}O$ occurs for column densities of a few 10^{15} cm^{-2}, and even $^{13}C^{16}O$ appears to be self shielded when $N(^{12}C^{16}O)$ is about 10^{16} cm^{-2}. Isotope charge exchange also favors diffuse molecular clouds with $N(^{12}C^{16}O)$ of a few $\times 10^{15}$ cm^{-2}. Millimeter-wave absorption against background active galactic nuclei, however, reveals clouds where isotope charge exchange dominates, but for $^{12}C^{16}O$ column densities between 1 and 2 $\times 10^{16}$ cm^{-2} (Liszt & Lucas 1998). This material has CO excitation temperatures (T_{ex}) of about 6 K (Liszt & Lucas 1998), while the sample in Sheffer *et al.* (2007) typically has T_{ex} of 4 K. This difference suggests that the gas probed by millimeter-wave absorption may have somewhat larger gas densities; larger gas densities could also yield the richer molecular chemistry observed for the millimeter-wave sample (e.g., Lucas & Liszt 2000; Liszt & Lucas 2001).

Recent measurements on the $^{12}CH^+/^{13}CH^+$ and $^{12}C^{14}N/^{13}C^{14}N$ ratios (Ritchey *et al.* 2011) provide complementary information on CO fractionation. Non-thermal conditions seem necessary for CH$^+$ synthesis in diffuse molecular gas (e.g., Federman *et al.* 1996a; Godard *et al.* 2009). As a result, the $^{12}CH^+/^{13}CH^+$ ratio is expected to trace the ambient $^{12}C/^{13}C$ ratio. Ritchey *et al.* (2011) obtained a weighted average of 74.4 ± 7.6 for their sample, with no evidence for variation among sight lines. This ratio is indistinguishable from the dark cloud value in the solar neighborhood.

The analyses of Pan *et al.* (2005), Sonnentrucker *et al.* (2007), and Sheffer *et al.* (2008) indicate a close correspondence between the component structures (velocities, *b*-values, and relative component strengths) derived from CN and CO. This suggests that both molecules sample the densest portions of diffuse molecular material. A consequence of the correspondence relates to fractionation. Since CO is the most abundant C-bearing molecule, it plays a key role in the partitioning of ^{12}C and ^{13}C in other C-bearing species. If an enhancement in $^{12}C^{16}O(^{13}C^{16}O)$ is present, one would expect that the reservoir for $^{12}C(^{13}C)$ is depleted and that carbon species other than CO show the opposite fractionation. The interpretation of the observed $^{12}C^{14}N/^{13}C^{14}N$ ratio has to involve C$^+$, the most abundant form of carbon in diffuse molecular clouds (Ritchey *et al.* 2011). Their analysis indicated that between 10 and 50% of the elemental carbon is in CO for the material probed by $^{12}C^{16}O/^{13}C^{16}O$ and $^{12}C^{14}N/^{13}C^{14}N$.

Accurate oscillator strengths (*f*-values) are needed to derive meaningful CO column densities from observations and to model the self shielding process. Spectra acquired with the *Hubble Space Telescope* reveal CO absorption from the $A - X$ system of bands as well as weaker triplet-singlet bands ($a' - X$, $d - X$, and $e - X$). Self-consistent sets of *f*-values are now available for these bands. For the $A - X$ bands, *f*-values obtained from electron scattering (Chan *et al.* 1993), laser absorption (Stark *et al.* 1998), and synchrotron absorption (Eidelsberg *et al.* 1999) agree very well. Similarly, agreement between astronomical *f*-values (e.g., Sheffer *et al.* 2002a) and theoretical values (Eidelsberg & Rostas 2003) for triplet-singlet transitions is now excellent, better than 1σ in most instances.

Sheffer *et al.* (2003) detected several Rydberg bands of CO that were thought to be important for its photochemistry (van Dishoeck & Black 1988) toward HD 203374A with the *Far Ultraviolet Spectroscopic Explorer* and derived *f*-values for the bands. Their *f*-values for the $B - X$ (0,0), $B - X$ (1,0), and $E - X$ (0,0) bands agree with those determined by Federman *et al.* (2001) using synchrotron radiation. Our more recent synchrotron-based experiments (Eidelsberg *et al.* 2004, 2006, 2012) confirm the values for the other bands analyzed by Sheffer *et al.* (2003). The laboratory effort is continuing
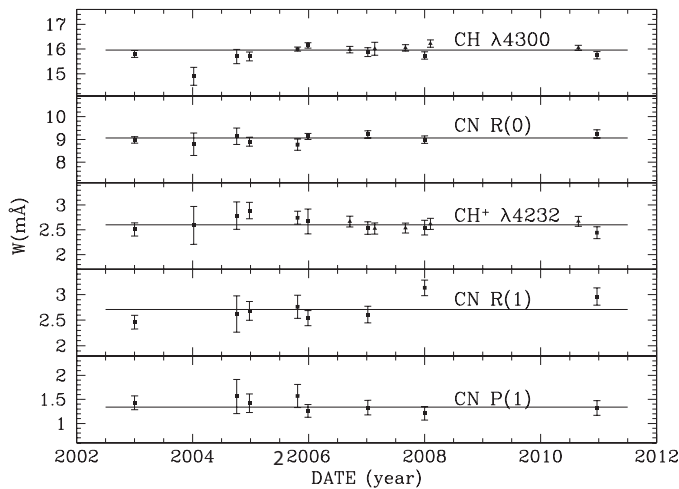
Figure 1. Equivalent width of the CN P(1) line, the CN R(1) line, CH$^+$ λ4232, the CN R(0) line, and CH λ4300 toward ζ Per between 2003 and 2011. The filled squares correspond to data acquired at the 2.7 m telescope at McDonald Observatory, and filled triangles represent data from Observatoire de Haute-Provence. The horizontal lines indicate the weighted average for each molecular feature. (See Boissé *et al.* 2013 for details.)

with data acquired at the SOLEIL synchrotron; measurements are being made on several isotopologues and include the derivation of predissociation rates needed in models.

3. Small-scale Structure

Rollinde *et al.* (2003) and Boissé *et al.* (2009) studied the small-scale structure toward the runaway star AE Aur through observations of CH$^+$ and CH absorption. Instrumental stability was checked through measurments on ζ Per, whose proper motion is much smaller and whose interstellar spectra did not appear to vary. We continued to monitor absorption toward the latter star and now find evidence for variations in the equivalent width and b-value of the CH$^+$ line at 4232 Å (Boissé *et al.* 2013, in preparation). In particular, the relative change in CH$^+$ column density ($\delta N/N$) over a 3 year period is 10%, while the limits for changes in CH and CN columns are less than 6%. Figure 1 highlights the observed variation in CH$^+$ equivalent width compared to those of CH and CN lines, and Figure 2 shows that the apparent variation in equivalent width and b-value occurs over the same timeframe.

These results place interesting constraints on CH$^+$ formation mechanisms. Over a 3-year interval, ζ Per travels about 10 AU across the sky. The change in CH$^+$ column density is about 4×10^{11} cm^{-2}, and the limit for the change in N(CH) is 3×10^{11} cm^{-2}. The length scale of 10 AU is much smaller than widths of typical interstellar shocks (Flower & Pineau des Forêts 1998), suggesting that shocks are not playing a role here. Heat produced by vorticies are another possibility (Godard *et al.* 2009). For a gas density of 100 cm^{-3}, the above changes in column density would suggest that approximately 10 vortices crossed the line of sight between 2004 and 2007.

4. Absorption from OH$^+$ and OH

We conducted a survey of molecular absorption from diffuse interstellar clouds and here describe the results pertaining to OH$^+$ and OH lines in the near ultraviolet. Porras
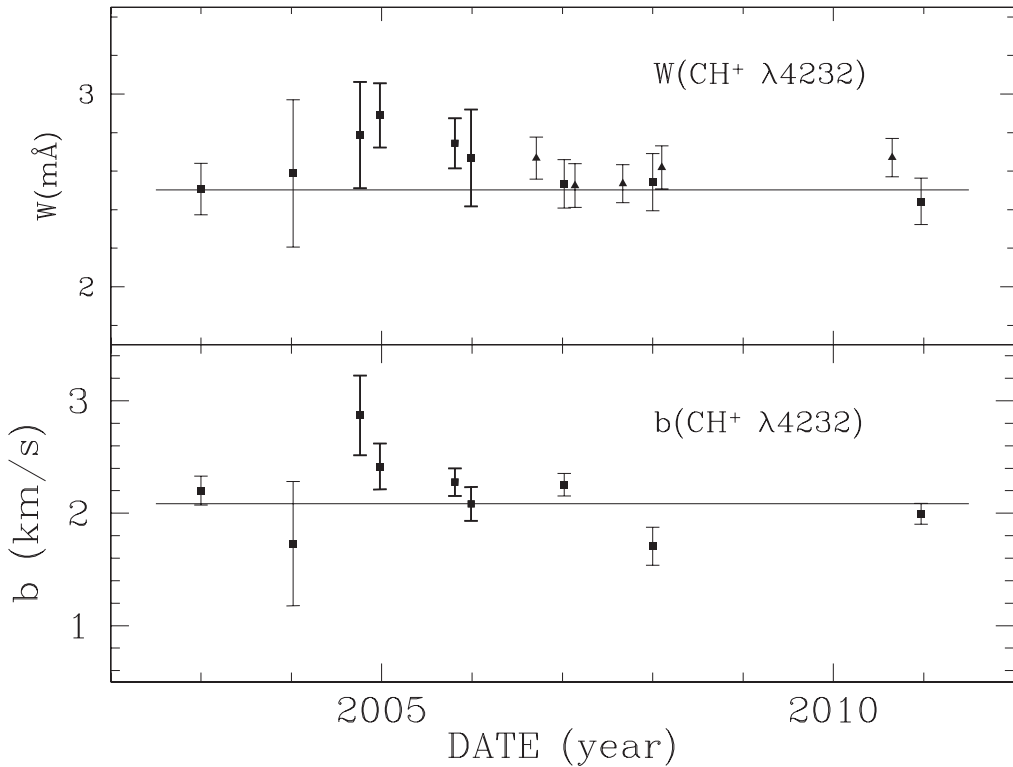
Figure 2. Time variation of the *b*-value (derived from only the high-resolution spectra from McDonald Observatory) and equivalent width for CH$^+$ $\lambda 4232$ toward ζ Per between 2003 and 2011. (See Boissé *et al.* 2013 for details.)

et al. (2013) focused on the directions toward BD$-14°$ 5037, HD 149404, HD 154368, and HD 183143, where different components have different relative abundances. In particular, OH$^+$ absorption is strongest in components with large CH$^+$ abundances, especially relative to the amount of CH present. The strongest OH absorption is associated with gas containing significant amounts of CN. Figure 3 reveals these correspondences for diffuse molecular gas toward BD$-14°$ 5037.

Porras *et al.* interpreted these results in the following way. Because CH$^+$ is rapidly destroyed by reactions with H and H$_2$ (as well as electrons), it is observed in relatively low density gas with small molecular hydrogen fractions. These conditions must also pertain to OH$^+$ detections. The findings are consistent with the analysis of sub-millimeter wave observations of OH$^+$, H$_2$O$^+$, and H$_3$O$^+$ absorption toward star-forming regions with the *Herschel Space Telescope* (Neufeld *et al.* 2010). They also confirm the statement by Krełowski *et al.* (2010) that OH$^+$ absorption at near ultraviolet wavelengths is associated with CH$^+$ features. On the other hand, CN is believed to trace denser gas with significant amounts of H$_2$ (e.g., Pan *et al.* 2005). Since OH is produced from OH$^+$ via additional reactions involving H$_2$ (see above), its correspondence with components rich in CN is understandable.

Porras *et al.* (2013) also performed simple chemical analyses based on the scheme presented in Federman *et al.* (1996b) in order to extract the cosmic ray ionization rate. Only charge exchange with protons and O atoms was considered because OH$^+$ is detected in low density gas. The conditions adopted for the material detected in OH$^+$ were
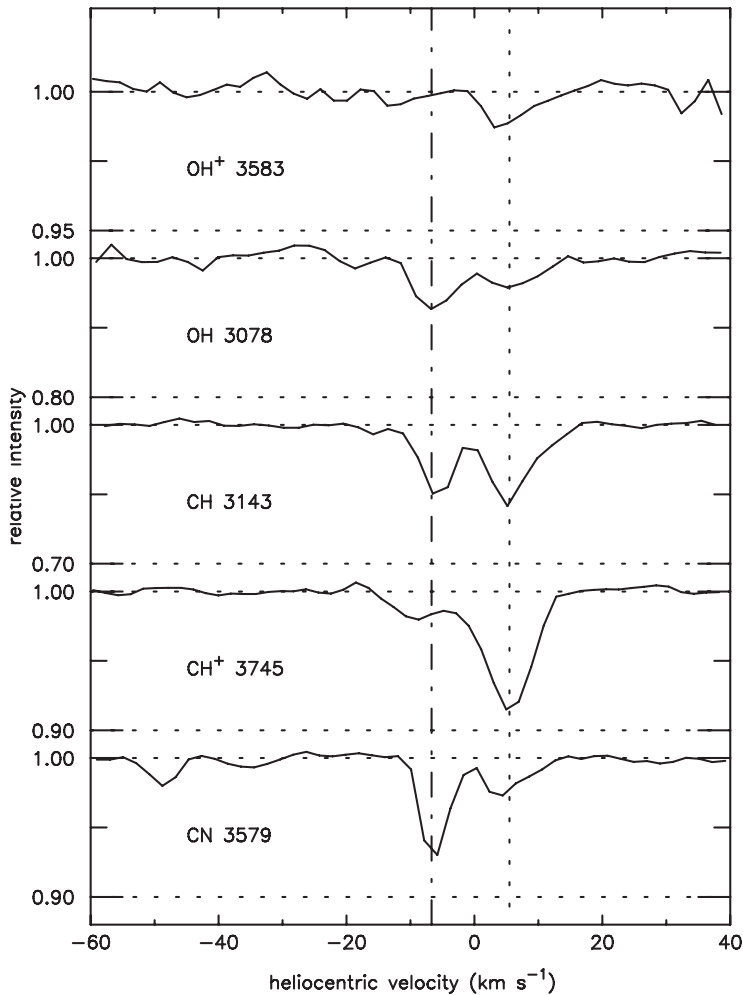
Figure 3. Absorption from OH^+, OH, CH, CH^+, and CN toward $BD-14°$ 5037. The wavelengths of each feature are indicated. The feature near -50 km s^{-1} is the CN R(1) line. Note that the vertical scales differ from panel to panel. The dotted vertical line highlights the main CH^+/OH^+ component, while the dot-dashed line indicates the main CN/OH components. (See Porras *et al.* 2013 for details.)

a gas density of 100 cm^{-3}, a temperature of 80 K, and a fractional abundance of atomic hydrogen 10 times larger than that for H$_2$. For the OH components, the respective quantities were 300 cm^{-3}, 50 K, and equal amounts of H and H$_2$. Considering the simplicity of the modeling, it is somewhat surprising that the primary cosmic ray ionization rate for all components seen toward the 4 stars appears to be about 10^{-16} s^{-1}. Similar values for the rate were found by Neufeld *et al.* (2010) and Indriolo & McCall (2012) in their studies of diffuse molecular clouds. It is not unexpected that the rate is the same for the components seen in both OH^+ and OH, but this highlights the fact that even diffuse clouds show variations in the physical conditions with depth.

5. Molecular Excitation

Individual rotational levels are observed for H_2, CO, CN, C_2, and C_3. The amount of excitation provides information on gas density, gas temperature, the strength of the radiation field permeating the clouds and in some instances the process of molecule formation. As discussed above, the different values for T_{ex} seen in ultraviolet and millimeter-wave observations of CO may provide insight into the relationship between the clouds detected by these techniques. Excitation among CN levels yields an upper limit on the temperature of the cosmic background radiation (e.g., Roth & Meyer 1995). Recent measurements (e.g., Ritchey *et al.* 2011) indicate that for some directions, collisions within the gas cloud also have to be considered; Black & van Dishoeck (1991) studied electron excitation in detail. (The large fractional abundance of C^+ in diffuse molecular clouds provides the necessary electrons.)

Absorption from many rotational levels in H_2, C_2, and C_3 is observed, with the lowest lying levels having a distinctly lower excitation temperature than the T_{ex} associated with intermediate and high-lying levels. For H_2, measurements for $J = 0$ and 1 provide an estimate of the gas temperature (e.g., Savage *et al.* 1977). For $J \geqslant 2$, the excitation can arise from a combination of absorption of ultraviolet photons followed by cascades within ro-vibrational levels of the ground electronic state, collisions within shocks, and the excess energy available during H_2 formation. Early analyses of H_2 excitation in diffuse molecular clouds were based on *Copernicus* results (Jura 1974, 1975a, b). More recent studies include Meyer *et al.* (2001), Gry *et al.* (2002), and Boissé *et al.* (2005); it is noteworthy that Meyer *et al.* and Boissé *et al.* detected vibrationally excited H_2 and modeled these observations as well. Analysis of C_2 excitation reveals the gas temperature from the column densities for low lying levels and the strength of the infrared radition field and gas density from higher lying ones (van Dishoeck & Black 1982). Over the intervening years, updated collisional rates and oscillator strengths have become available. These new data were incorporated into a model of C_2 excitation by Casu & Cecchi-Pestellini (2012), and Hupe *et al.* (2012) described the changes caused by adopting the newest results. As for C_3 excitation, the most detailed analysis to date is that of Roueff *et al.* (2002) based on observations for the gas toward HD 210121. They modeled the absorption by considering gas density, gas temperature, the far infrared radiation field, and the formation process.

These examples reveal that molecular (and atomic) excitation provides complementary information on conditions for diffuse molecular clouds.

6. Constraining Models

In Sections 2 through 5, relatively recent observations of diffuse molecular clouds, with a bias toward those at ultraviolet and visible wavelengths, were described. The sight lines are among the many used to measure the properties of Diffuse Interstellar Bands. I conclude by suggesting how the observational constraints can lead to improved detailed models for this environment.

The measurements discussed above offer a number of avenues for further study.

• Photochemistry governs molecular abundances and fractionation among CO isotopologues. Current models have difficulty reproducing the large $^{12}C^{16}O/^{13}C^{16}O$ ratios seen in gas toward stars in Ophiuchus. The precise oscillator strengths and predissociation rates coming from ongoing experiments may hold the key.

• New observations of OH^+ and OH indicate that distinct pathways produce CH^+ and OH. Essentially all the observed OH seems to come from cosmic ray ionization, not material with elevated temperatures.

• The OH^+ and OH results also indicate that modeling efforts need to focus on specific components along the line of sight and need to allow conditions to vary with depth into a cloud.

• Molecular (and atomic) excitation should be incorporated into the models as well. This will help constrain the range in physical conditions with depth. Analysis of excitation may also reveal the connection between gas observed via different techniques.

These improvements are likely to lead to a deeper understanding of the processes taking place in diffuse molecular clouds.

Acknowledgements

References

Bally, J. & Langer, W. D. 1982, *ApJ*, 255, 143
Black, J. H. & Dalgarno, A. 1977, *ApJS*, 34, 405
Black, J. H. & van Dishoeck, E. F. 1991, *ApJ*, 369, L9
Boissé, P., Federman, S. R., Pineau des Forêts, G., Ritchey, A. M., & Sheffer, Y. 2013, *A&A*, 559, A131
Boissé, P., Le Petit, F., Rollinde, E., *et al.* 2005, *A&A*, 429, 509
Boissé, P., Rollinde, E., Hily-Blant, P., *et al.* 2009, *A&A*, 501, 221
Casu, S. & Cecchi-Pestellini, C. 2012, *ApJ*, 749, 48
Chan, W. F., Cooper, G., & Brion, C. E. 1993, *Chem. Phys.*, 170, 123
Eidelsberg, M., Jolly, A., Lemaire, J. L., *et al.* 1999, *A&A*, 346, 705
Eidelsberg, M., Lemaire, J. L., Federman, S. R., *et al.* 2012, *A&A*, 543, A69
Eidelsberg, M., Lemaire, J. L., Fillion, J. H., *et al.* 2004, *A&A*, 424, 355
Eidelsberg, M. & Rostas, F. 2003, *ApJS*, 145, 89
Eidelsberg, M., Sheffer, Y., Federman, S. R., *et al.* 2006, *ApJ*, 647, 1543
Federman, S. R., Fritts, M., Cheng, S., *et al.* 2001, *ApJS*, 134, 133
Federman, S. R., Lambert, D. L., Sheffer, Y., *et al.* 2003, *ApJ*, 591, 986
Federman, S. R., Rawlings, J. M. C., Taylor, S. D., & Williams, D. A. 1996a, *MNRAS*, 279, L41
Federman, S. R., Weber, J., & Lambert, D. L. 1996b, *ApJ*, 463, 181
Flower, D. R. & Pineau des Forêts, G. 1998, *MNRAS*, 297, 1182
Glassgold, A. E. & Langer, W. D. 1974, *ApJ*, 193, 73
Glassgold, A. E. & Langer, W. D. 1976, *ApJ*, 206, 85
Godard, B., Falgarone, E., & Pineau des Forêts, G. 2009, *A&A*, 495, 847
Gry, C., Boulanger, F., Nehmé, C., *et al.* 2002, *A&A*, 391, 675
Hupe, R. C., Sheffer, Y., & Federman, S. R. 2012, *ApJ*, 761, 38
Indriolo, N. & McCall, B. J. 2012, *ApJ*, 745, 91
Jura, M. 1974, *ApJ*, 191, 375
Jura, M. 1975a, *ApJ*, 197, 575
Jura, M. 1975b, *ApJ*, 197, 581
Krełowski, J., Beletsky, Y., & Galazutdinov, G. A. 2010, *ApJ*, 719, L20
Lambert, D. L., Sheffer, Y., Gilliland, R. L., & Federman, S. R. 1994, *ApJ*, 420, 756
Liszt, H. S. & Lucas, R. 1998, *A&A*, 339, 561
Liszt, H. S. & Lucas, R. 2001, *A&A*, 370, 576
Lucas, R. & Liszt, H. S. 2000, *A&A*, 355, 327
Meyer, D. M., Lauroesch, J. T., Sofia, U. J., Draine, B. T., & Bertoldi, F. 2001, *ApJ*, 553, L59
Neufeld, D. A., Goicoechea, J. R., Sonnentrucker, P., *et al.* 2010, *A&A*, 521, L10

Pan, K., Federman, S. R., Sheffer, Y., & Andersson, B-G 2005, *ApJ*, 663, 986

Porras, A. J., Federman, S. R., Welty, D. E., & Ritchey, A. M. 2013, *ApJ Letters*, 781, 8

Ritchey, A. M., Federman, S. R., & Lambert, D. L. 2011, *ApJ*, 728, 36

Rollinde, E., Boissé, P., Federman, S. R., & Pan, K. 2003, *A&A*, 401, 215

Roth, K. C. & Meyer, D. M. 1995, *ApJ*, 441, 129

Roueff, E., Felenbok, P., Black, J. H., & Gry, C. 2002, *A&A*, 384, 629

Savage, B. D., Bohlin, R. C., Drake, J. F., & Budich, W. 1977, *ApJ*, 216, 291

Sheffer, Y., Federman, S. R., & Andersson, B.-G. 2003, *ApJ*, 597, L29

Sheffer, Y., Federman, S. R., & Lambert, D. L. 2002a, *ApJ*, 572, L95

Sheffer, Y., Lambert, D. L., & Federman, S. R. 2002b, *ApJ*, 574, L171

Sheffer, Y., Rogers, M., Federman, S. R., Lambert, D. L., & Gredel, R. 2007, *ApJ*, 667, 1002

Sheffer, Y., Rogers, M., Federman, S. R., *et al.* 2008, *ApJ*, 687, 1075

Sonnentrucker, P., Welty, D. E., Thorburn, J. A., & York, D. G. 2007, *ApJS*, 168, 58

Stark, G., Lewis, B. R., Gibson, S. T., & England, J. P. 1998, *ApJ*, 505, 452

van Dishoeck, E. F. & Black, J. H. 1982, *ApJ*, 258, 533

van Dishoeck, E. F. & Black, J. H. 1986, *ApJS*, 62, 109

van Dishoeck, E. F. & Black, J. H. 1988, *ApJ*, 334, 771

Visser, R., van Dishoeck, E. F., & Black, J. H. 2009, *A&A*, 503, 323

Watson, W. D., Anicich, V. G., & Huntress, W. T., Jr. 1976, *ApJ*, 205, L165

Wilson, T. L. 1999, *Rep. Prog. Phys.*, 62, 143